

Sensitivity Analysis for Scenarios Relevant to Evolution of Overpack and Buffer Material *-11176

Seiji Takeda, Masatoshi Watanabe and Hideo Kimura
Nuclear Safety Research Center, Japan Atomic Energy Agency (JAEA),
Tokai, Ibaraki, 319-1195 Japan

ABSTRACT

This study focuses on a deterioration of expected barrier functions relevant to evolution of overpack and sand-bentonite buffer material in engineered barrier system in the geological disposal of high-level radioactive waste. Release rates for important radionuclides, Cs-135 and Se-79, were estimated from Monte Carlo-based analysis for the early failure of overpack and the buffer alteration scenarios. One of the possible early failure scenarios is the change of glass dissolution rate, effective diffusion coefficients and distribution coefficients in the buffer material, which are affected by early high temperature in the engineered barrier. The analytical result indicates that this scenario has no detrimental effect on the maximum release rates of these radionuclides. Another scenario is the occurrence of the increase of Se solubility correlated with the enhanced redox potential due to the radiolysis after the early failure of overpack. This scenario allows a conspicuous increase in the maximum release rates of Se-79 from the buffer, which is over one order of magnitude higher than that in the normal scenario. In addition, with the comparison of the maximum release rates between the early failure scenario and the buffer alteration scenario, it is suggested that the effect of the deterioration of the expected barrier functions relevant to the buffer alteration on the release rates is more remarkable than the effect on early failure.

INTRODUCTION

Nuclear Safety Research Center (NSRC) of Japan Atomic Energy Agency (JAEA) has carried out regulatory research to provide technical support for safety review of the license application for candidate sites of final disposal of high-level radioactive waste (HLW), which Nuclear Waste Management Organization of Japan (NUMO) as an implementer will propose through the stepwise setting process [1]. Our regulatory research is to develop tools (scenarios, models and parameters) to assess the long-term performance of a geological disposal system. In safety assessment for a geological disposal of HLW, it is of consequence to estimate the uncertainties due to the long time frame associated with long-lived radionuclides and the expanded geological environment. This study focuses on a deterioration of expected barrier functions relevant to evolution of overpack and sand-bentonite buffer material in engineered barrier system.

For carbon steel as a candidate material of overpack, one of its main functions is isolation of vitrified wastes from groundwater in the barrier system. In the H12 Project report published by Japan Nuclear Cycle Development Institute (JNC), general corrosion was estimated as the main mode of corrosion and the lifetime of isolation could be expected to be at least 1,000y [2]. However, carbon steel is likely to be attacked by local corrosion under groundwater chemistries such as highly alkaline groundwater from cementitious materials as a plug or grout [3], or attacked by stress corrosion cracking under a particular

* This study is regulatory support research funded by the Nuclear and Industrial Safety Agency (NISA), Ministry of Economy, Trade and Industry (METI).

potential condition such as an active-passive transition in carbonate-bicarbonate solution [4] [5]. The occurrence of this corrosion can be related to early failure of the function of isolation. Maeda et al. [6] have been developing the model and code to evaluate the overpack lifetime associated with the occurrence and progress of these corrosion phenomena.

Alteration of the buffer material (70 wt% bentonite and 30 wt% sand) may progress during the period of elevated temperatures and/or under highly alkaline environments induced by cementitious materials. The long-term alteration of buffer material may have detrimental effects on its physical or chemical properties. The deterioration of impermeability and/or low diffusivity caused by the alteration, which are expected as main functions of the buffer, may be considered to affect radionuclide migration from vitrified wastes to a host rock. Variation of the hydraulic conductivity caused by the alteration is considered to affect the mass transport from glass to the host rock. Nakayama et al. [7] and Yamaguchi et al. [8] in our research group have modeled the hydraulic conductivity of compacted sand–bentonite mixtures through their experiments on montmorillonite dissolution under alkaline conditions.

It is supposed that some kinds of variation of properties or process in the overpack and the buffer result in the potential loss of their main functions. In this study, release rate from the buffer for important radionuclides, Cs-135 and Se-79, were estimated for the scenario of the deterioration of the expected barrier functions relevant to evolution of the overpack and the buffer, in order to identify important variation of properties or process and their related parameters accompanied with the early failure of overpack and the alteration of buffer.

SCENARIO DESCRIPTION

In this analysis, disposal site is not specific, and geological disposal system is basically the same design as in the H12 Project report [2] of Japan Nuclear Cycle Development Institute. The repository is constructed in a stable granitic bedrock at a depth of 1,000 m. The rock is described in terms of two major hydraulic units; fractured zone and rock mass. It is reasonable to assume that the repository is constructed in a stable rock mass having enough distances from fractured zones, in order to avoid the occurrence of a short path of groundwater from the repository to the biosphere.

The engineered barrier system is composed of borosilicate vitrified waste form, carbon steel overpack and bentonitic buffer material (a mixture of 70 wt% of bentonite and 30 wt% of sand). Cementitious materials are used for the plugs, grouting and support of tunnel. Total number of the vitrified waste canisters is 40,000 [2].

Four analytical cases are set as shown in Table I. In the normal scenario (Case A), it is assumed that no advertent events are anticipated and radionuclides are transported in the intact geological disposal system. Two kinds of the cases (Case B1 and Case B2) are considered for the scenario on the early failure (<1,000 y) of overpack. The Case B1 leads to the effects of early high temperature (about 90 degrees) on glass dissolution rate, effective diffusion coefficient and distribution coefficient in the buffer. Additionally, the case B2 assumes that radiolysis of groundwater, which is caused by gamma and alpha radiation with early migration of radionuclides into engineered barrier, brings about increased redox potential by radiolytic oxidants, and resulting enhanced solubility limit for radionuclides. The possibility of loss of its isolation function at less than 1,000 y is supposed to be low. In the analysis for Case B1 and Case B2, it is assumed that the number of the vitrified waste canisters suffering from the early failure of overpack is 8,000 conservatively, which corresponds to 20 % of total waste canisters (40,000).

On the basis of our previous sensitivity analysis [9], the possible alternation scenario of bentonitic buffer

material is selected as the loss of impermeability and the occurrence of advective groundwater flow in the altered buffer material, and resulting increased glass dissolution rate. This case of alteration scenario is referred to as Case C.

Table I Description of normal, early failure and alteration scenarios targeted in this analysis

Scenario	Description	Case
Normal scenario	No advertent events are anticipated and radionuclides are transported in the intact geological disposal system.	Case A
Early failure scenario	Early failure (<1,000y) of overpack leads to the effects of higher temperature to increased effective diffusion coefficient and glass dissolution rate than them in normal scenario.	Case B1
	Additionally, it is assumed that radiolysis of groundwater due to gamma and alpha radiation with early migration of radionuclides into engineered barrier brings about increased redox potential by radiolytic oxidants, and resulting enhanced solubility in it for radionuclides.	Case B2
Alteration Scenario	Advective transport of radionuclides is dominant, and advection of groundwater decreases the concentration of silica in the porewater in the buffer material, resulting in increased glass dissolution.	Case C

ANALYTICAL METHOD

Takeda et al. have developed the probabilistic safety assessment code system GSRW-PSA (Generic Safety assessment code for geologic disposal of Radioactive Waste Probabilistic Safety Assessment) [10], to quantify the uncertainties in parameters and conceptual models based on the Monte Carlo calculation. A compartment model of 1-D radionuclide transport in the engineered barrier system of GSRW-PSA is applied to this analysis. In normal scenario and alteration scenario of the buffer, it is assumed that the isolation function of overpack for 40,000 vitrified waste canisters is lost at 1,000 y. In the early failure scenario, its isolation function of both 8,000 waste canisters and the others (32,000) is lost at 100 y and at 1,000 y, respectively. After the overpack failure, radionuclides are released from the vitrified waste form as a result of glass matrix dissolution. Radionuclides are transported in the overpack and buffer material by diffusion and/or advection depending on the progress of the long-term alteration of the buffer material. Retardation and precipitation/dissolution determined by the elemental solubility were taken into account. The sorption onto the overpack is conservatively disregarded. The mathematical models of the congruent release with glass dissolution and the radionuclide migration in the overpack and the buffer material are described in our previous paper [9].

The time dependence of glass dissolution rate, diffusion coefficient, solubility, distribution coefficient, and/or velocity in the buffer material is considered in the early failure scenario and the alteration scenario. Those parameters are expressed as the step functions of time in GSRW-PSA. It is assumed that there is no spatial variation of the parameters in the buffer material.

The authors investigate the relationship between the maximum release rate of radionuclides discharged from the engineered barrier system and the time-dependent parameters, through the Monte Carlo calculation.

ESTIMATION OF PARAMETER UNCERTAINTY

The parameters on the design of the engineered barrier system are referred from the H12 Project report [2]. The uncertainties on five kinds of the parameters, i.e. solubility, glass dissolution rate, effective diffusion coefficient, distribution coefficient and pore velocity in the buffer material are considered in this analysis for three kinds of scenarios as shown in Table I.

Solubility

The solubility for Se is estimated using the probabilistic analysis code of uncertainty of solubility limit for radioactive elements in a geological disposal (PASOL), developed by Takeda et al. [11]. The PASOL computer code is based on the Latin Hypercube Sampling (LHS) code [12] and geochemical code of EQ3/6 [13]. The chemical composition of groundwater is taken from the calculated bentonite porewater in the H12 Project report [2]. The uncertainties of thermodynamic data of Se are basically referred from the uncertainty estimates that are represented in the NEA TDB [14]. The solid phase of Se solubility limiting is assumed to be Se(cr) based on the recent experiment of Se solubility [15]. The result of solubility calculation indicates that the uncertainty on solubility of Se(cr) is governed by the error of the equilibrium constant for the reaction between Se(cr) and HSe^- and estimated to be in the range of $1\text{E-}7$ to $6\text{E-}7$ mol/l corresponding to the 95% confidence intervals. This uncertainty of Se solubility is used for the normal scenario (Case A) and the alteration scenario (Case C).

Since crystallinity is generally enhanced by higher temperature in the early failure scenario, it is supposed that the solubility of Se(cr) tends to decrease under early high temperature. The effect of higher temperature on Se solubility is ignored conservatively. The calculated variation of Se solubility mentioned above is used for the early failure scenario (Case B1).

The radiolysis of groundwater in the engineered barriers may bring about the enhanced redox potential by radiolytic oxidants and lead to the increase of Se solubility. In the case of this state (Case B2), it is assumed that there is no solubility limit of Se conservatively.

Since Cs is a highly soluble element, the solubility limit for Cs is not considered for all analytical cases.

Glass Dissolution Rate

It is assumed that the alteration and dissolution of glass in the engineered barrier system proceeds by a mechanism neglecting the effects of the chemical affinity for dissolution reaction of glass matrix. The uncertainty of the long-term glass dissolution rate represented by a constant dissolution rate is estimated from the published data of glass dissolution. The statistical analysis of the release rate data of boron for the hypothetical condition of disposal system was performed to estimate the uncertainty [16]. The conditions for data selection are a type of glass, temperature, pH, ionic strength, and saturation condition of dissolved silica. As a result of the constant dissolution rate, the uncertainty of the glass dissolution rate is estimated to be a variation with about 3 orders ($0.0001 - 0.1$ g/m²/day) and logarithmic mean of 0.004 g/m²/day at 60 degrees. This variation of glass dissolution rate is used for the analytical case of the normal scenario. The probability density function of the glass dissolution rate is assumed to be a log-normal distribution. The parameter sets of glass dissolution rate in the Monte Carlo calculation are estimated by LHS code. The values for the following parameters are determined by the same method.

In the early failure scenario, the enhanced glass dissolution rate by temperature is in the range of 0.0003 to 0.3 g/m²/day, which is determined from the long-term glass dissolution rate data at 90 degrees. The time-dependence of glass dissolution rate is indicated in Fig.1. It is assumed that the dissolution rate keeps

constant at 90 degrees from 100 to 900 y, decreases after 900 y with the drop of temperature and becomes constant value at 60 degrees in the normal scenario after 1,000 y. Two kinds of glass dissolution rates before 900 y and after 1,000 y are determined by the LHS method as shown in Fig.1. The linear relation from 900 to 1,000 y is assumed.

Under the assumption of increased dissolution rate of the glass matrix correlated with the advective transport in the alteration scenario, it is supposed that the maximum of the dissolution rate is conservatively equivalent to the level of the first-order dissolution rate. The range of time-dependant glass dissolution rate is considered from 0.004 to 1.0 g/m²/day. Fig.1 depicts the relation between the increased dissolution rate and time. In the alteration scenario, it is assumed that the increase in glass dissolution rate (=0.004 g/m²/day) starts from 1,000 y after the disposal (t=0) as the alteration progresses and the end time for increased dissolution rate is in the variation of 2,000 to 10,000 y. The glass dissolution rate at the end time is determined by the LHS method. The probability density function of the end time is assumed to be a uniform distribution. The relation between the glass dissolution rate and time from the start to the end is assumed to be expressed by a linear function.

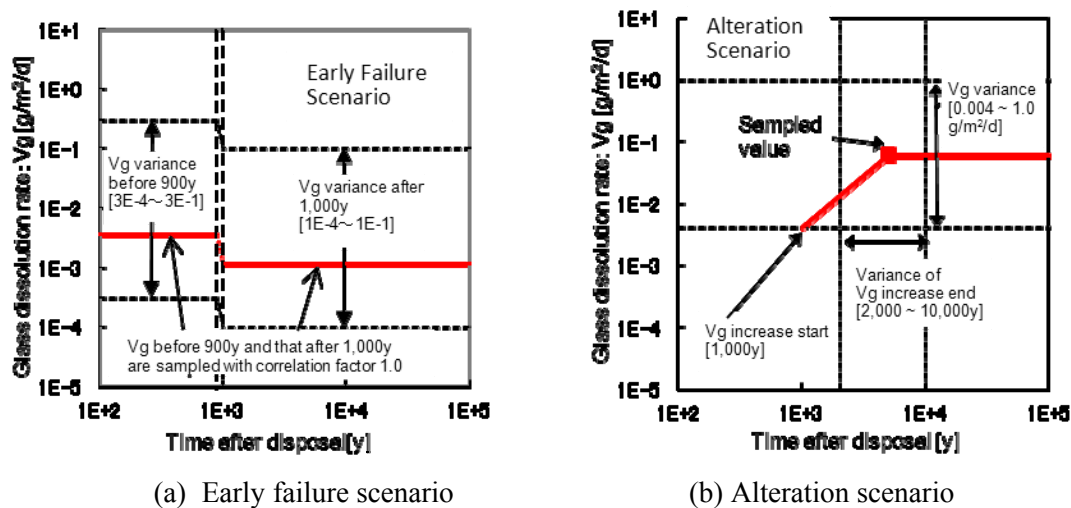


Fig.1 Time-dependence of glass dissolution rate for the early failure scenario of overpack and the alteration scenario of the buffer material

Effective diffusion coefficient in the buffer material

We estimate the uncertainty on the effective diffusion coefficients of Se and Cs in the buffer material through the statistical analysis for previous experimental data of the effective diffusion coefficient. The appropriate data are picked up based on the range of the density specification of montmorillonite gel. Additionally, under the assumption that the effective diffusion coefficient of Se may depend on an ionic strength, the data of Se are selected from the standard level of ionic strength for a fresh type groundwater. Table II shows the estimated variation of the effective diffusion coefficients of Se and Cs, which are corrected to the temperature of 60 and 90 degrees for the normal scenario and the early failure scenario, respectively. In the early failure scenario, it is assumed that the effective diffusion coefficients of Cs and Se keep constant at 90 degrees from 100 to 900 y, decrease after 900 y with the drop of temperature and become constant values at 60 degrees in the normal scenario after 1,000 y.

In the alteration scenario, since the dissolution of montmorillonite may lead to decreased density of montmorillonite gel, the effective diffusion coefficients of Se and Cs is likely to increase. Because of few data for bentonite alteration, the minimum values for Se and Cs are respectively based on the average values in the statistical analysis mentioned above, and the maximum values are conservatively given by the effective diffusion coefficients in free water. The probability density function of effective diffusion coefficient is assumed to be a log-normal distribution. The time-dependence of effective diffusion coefficient is basically treated in the same consideration mentioned in the selection of glass dissolution rate. In the alteration scenario, it is assumed that the increase in effective diffusion coefficient starts at 1,000 y after disposal ($t=0$) as the alteration progresses and the end time for increased diffusion coefficient varies from 2,000 to 10,000 y.

Table II Variation of effective diffusion coefficient in the buffer used in the calculations for normal scenario, early failure scenario and alteration scenario

parameter	scenario	element	unit	minimum ^{*1}	maximum ^{*1}
Diffusion coefficient in the buffer	Normal scenario	Cs	m ² /s	3E-11	1E-9
		Se		6E-12	1E-10
	Early failure scenario	Cs		5E-11 ^{*2}	2E-9 ^{*2}
		Se		1E-11 ^{*2}	2E-10 ^{*2}
	Alteration scenario	Cs		2E-10	4E-9
		Se		2E-11	4E-9

(*1)The minimum and maximum values are treated as the values of 0.1 percentile and 99.9 percentile in a log-normal distribution.

(*2) Specified when the time after disposal is less than 900 years. After 1,000 years, the same values as normal scenario are specified.

Distribution coefficient in the buffer material

The uncertainties on distribution coefficients in the buffer material are also estimated using the result of statistical analysis of them from previous experimental data. The variation of distribution coefficient is determined on the basis of the statistic, i.e. the average of measurements for compacted bentonite obtained from the in-diffusion method and the deviation of measurements from batch sorption tests. Moreover, the sorption data of Se are restricted to the reducing environment. Table III indicates the variations of distribution coefficients of Cs and Se for the normal scenario.

There is few sorption data for Cs and Se on temperature dependence for the early failure scenario. It is assumed that the variations of distribution coefficients for the early failure scenario are 0.1 times as low as those for the normal scenario and restricted to more than 1.0E-6 m³/kg. The distribution coefficients of Cs and Se keep constant from 100 to 900 y, increase after 900 y with the drop of temperature and become constant values in the normal scenario after 1,000 y.

The sorption property in the alteration of the buffer materials may deteriorate due to the dissolution of montmorillonite and mineralogical transformations. The sorption of the elements on the secondary minerals is conservatively ignored, and the variations of distribution coefficient for the alteration scenario are assumed to be the same for the early failure scenario. The probability density function of distribution

coefficient is assumed to be a log-normal distribution. The time-dependence of distribution coefficient is treated in the same consideration mentioned above. In the analysis for the alteration scenario, it is assumed that the decrease in distribution coefficient starts at 1,000 y after disposal as the alteration progresses and the end time for decreased distribution coefficient varies from 2,000 to 10,000 y.

Table III Variation of distribution coefficient used in the calculations for normal scenario, early failure scenario and alteration scenario

parameter	scenario	element	unit	minimum ^{*1}	maximum ^{*1}
Distribution coefficient in the buffer	Normal scenario	Cs	m ³ /kg	1E-3	1E+0
		Se		1E-6	3E-2
	Early failure scenario	Cs		1E-4 ^{*2}	1E-1 ^{*2}
		Se		1E-6 ^{*2}	3E-3 ^{*2}
	Alteration scenario	Cs		1E-4	1E-1
		Se		1E-6	3E-3

(*1)The minimum and maximum values are treated as the values of 0.1 percentile and 99.9 percentile in a log-normal distribution.

(*2) Spcified when the time after disposal is less than 900 years.After 1,000 years, the same values as normal scenario are spcified.

Pore velocity in the buffer material

Under the assumption of the deterioration of hydraulic conductivity due to the long-term alteration, the pore velocity in the altered buffer for the case of changing into advective transport is estimated from the 2-D groundwater flow and trajectory analysis for the buffer material and the near rock mass [8]. From the results of velocity analysis, the pore velocity in the altered buffer for the analytical case of advective transport is assumed to vary from 1E-4 to 1.0 m/y. A log-normal distribution for pore velocity is used and the time-dependence of pore velocity is treated in the same consideration mentioned above. It is assumed that the increase in pore velocity starts at 1,000 y after the disposal as the alteration progresses and the end time for increased pore velocity varies from 2,000 to 10,000 y.

The pore velocities in the analytical cases for the normal scenario and for the early failure scenario of overpack are considered as the result of velocity analysis under the hydraulic conductivity of 1E-12 m/s of the buffer material.

RESULTS AND DISCUSSION

The sensitivity analysis is conducted for 1,000 parameter sets with Monte Carlo technique. Fig.2 shows Se-79 release rate for 40,000 vitrified waste canisters with 100 sampling sets for the buffer changing with the lapse of time, comparing results for the normal scenario (Case A), for two analytical cases (Case B1 and B2) of early failure scenario and for the alteration scenario (case C). In Case B1 of the early failure scenario, the time profiles of Se-79 release rate before 100 y, considering the influence of early high temperature (90 degrees), are not higher than those after 1,000 y. In Case B2 of early failure scenario, however, the time profiles of Se-79 release rate before 100 y are enhanced by the specific factor of the radiolysis of groundwater due to gamma and alpha radiations with early migration of radionuclides. The result of Case C

for the alteration scenario indicates that the time-dependent variabilities of pore velocity, Se effective diffusion coefficient in the buffer and glass dissolution rate result in making the increased peak release rate of Se-79 after 2,000 y. The peak release rates of Se-79 for Case B2 and Case C tend to be higher than that for the normal scenario (Case A).

Fig.3 indicates the time profiles of Cs-135 release rate for 40,000 vitrified waste canisters with 100 sampling sets. The analytical case of Cs-135 for the early failure scenario is only Case B1, because no effect of the radiolysis of groundwater on Cs solubility was considered. In the result of CaseB1, the peak release rate of Cs-135 before 900 y correlated with the effect of high temperature on glass dissolution rate, Cs effective diffusion coefficient and Cs distribution coefficient due to early failure of overpack is equivalent to that after 1,000 y. The peak release rate of Cs-135 in the alteration scenario (Case C) is higher than that in the other scenarios due to the increase of glass dissolution rate and pore velocity accompanied with the alteration of buffer.

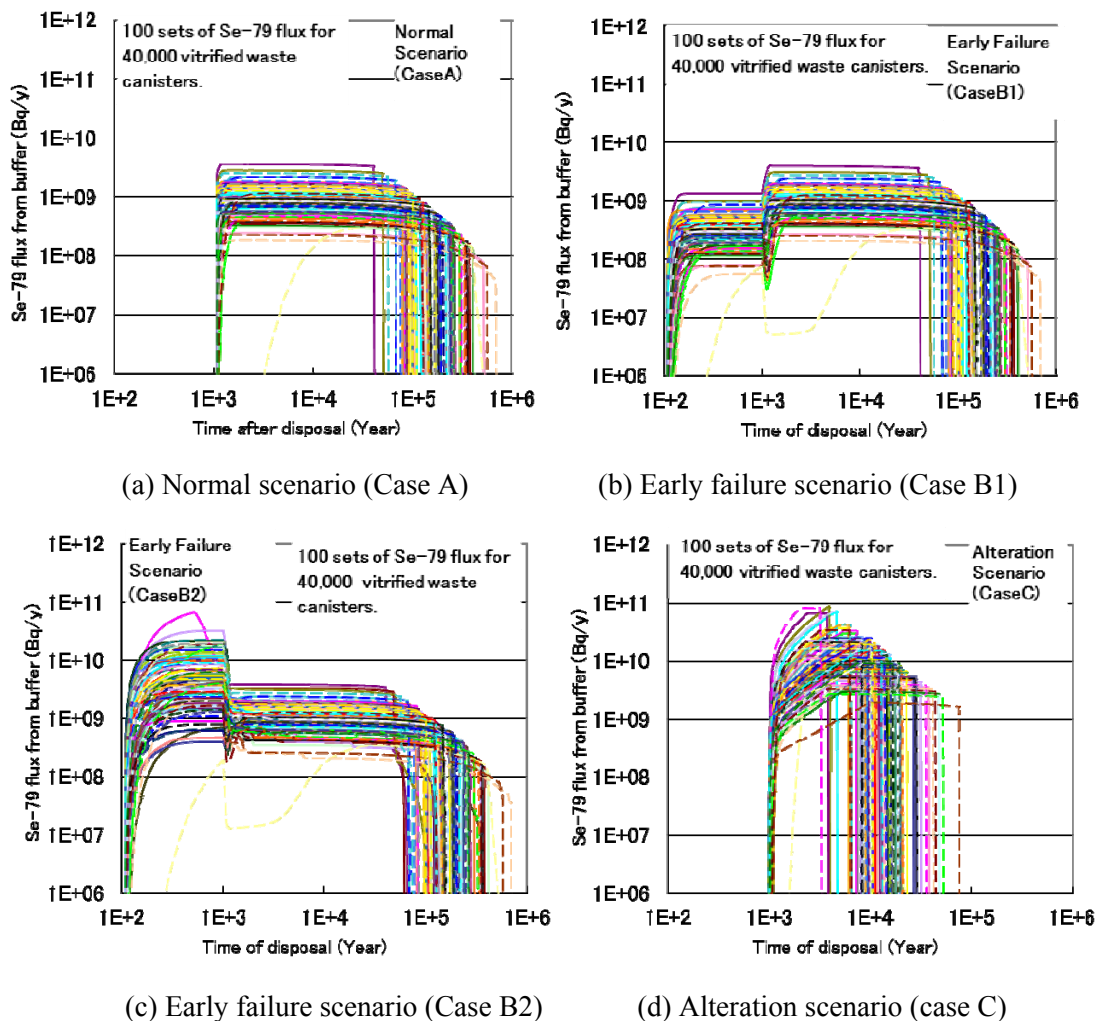


Fig.2 Results of sensitivity analysis of Se-79 for the normal scenario (Case A), for two analytical cases (Case B1 and B2) of early failure scenario and for the alteration scenario (Case C)

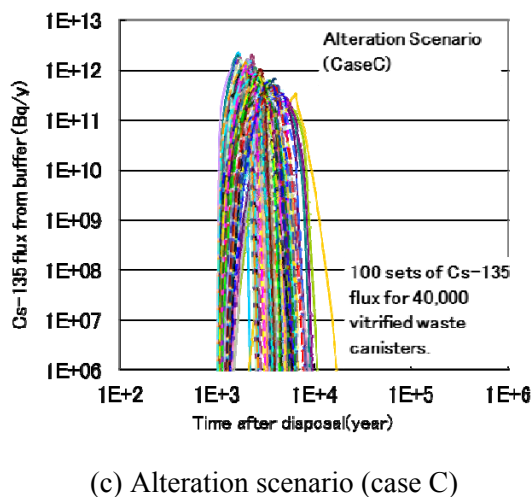
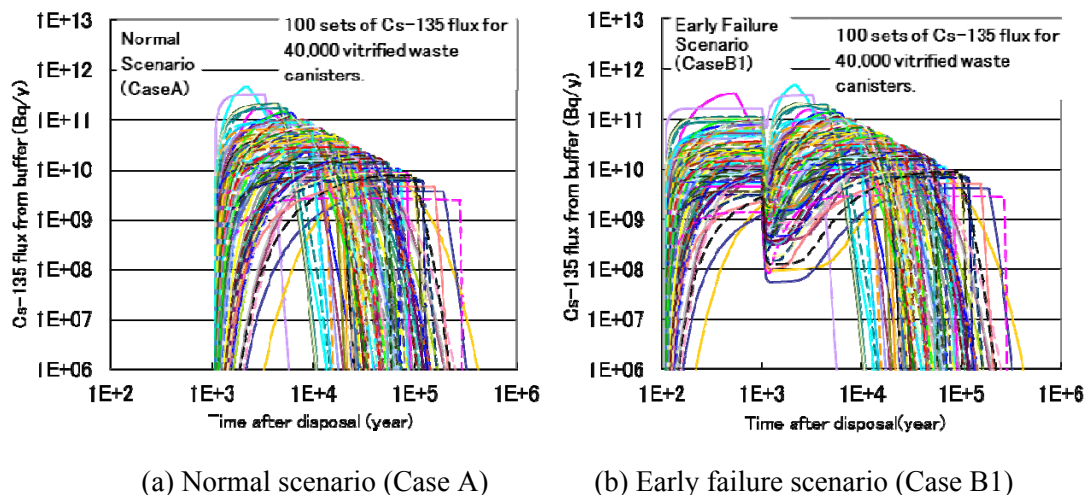


Fig.3 Results of sensitivity analysis of Cs-135 for the normal scenario (Case A), for the early failure scenario (Case B1) and for the alteration scenario (case C)

Fig.4 shows a comparison among complementary cumulative probabilities of Se-79 and Cs-135 maximum release rates for 40,000 vitrified waste canisters from the buffer for three kinds of scenarios. The 97.5th percentile of maximum release rate from the buffer material corresponding to the upper endpoint of the 95th percentile confidence interval is applied to an index for comparing those calculation results. The 97.5th percentile value of Se-79 in the case of the early failure scenario in response to the effect of high temperature (Case B1) is namely equivalent to that in Case A of the normal scenario. There is also little difference between the 95th percentile results of Cs-135 in Case A and CaseB1. Therefore, under the assumption of the early failure corresponding to 20 % of total waste canisters the high temperature of about 90 degrees with the early failure has no detrimental effect on the maximum release rates of Se-79 and Cs-135 from the buffer.

In addition, the 97.5th percentile value of Se-79 in CaseB2 of the early failure scenario under the additional condition of the increased Se solubility by the radiolysis is about one order of magnitude higher than that in Case A of the normal scenario. This result indicates that the increase of Se solubility correlated

with the enhanced redox potential due to the radiolysis in the early failure scenario makes a great effect on the maximum release rate of Se-79 from the buffer.

As shown in Fig.4, the 97.5th percentile values of Se-79 and Cs-135 in the alteration scenario of buffer (Case C) are the highest in all scenarios. These results suggest that the effect of the deterioration of the expected barrier functions relevant to buffer alteration to Se-79 and Cs-135 release rates is more remarkable than that with early failure of overpack.

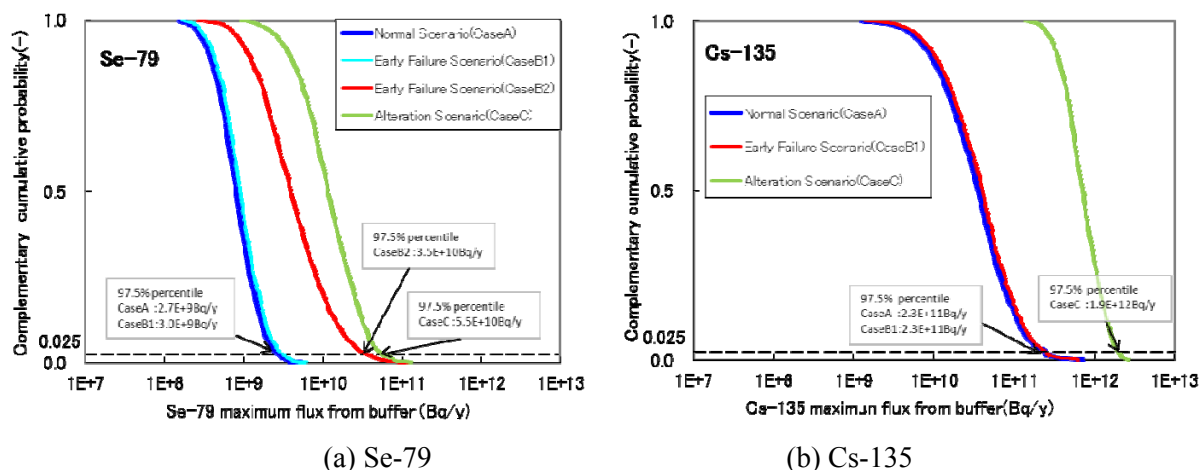


Fig.4 Comparison among complementary cumulative probabilities of Se-79 and Cs-135 maximum release rates per 40,000 vitrified waste canisters from the buffer for three kinds of scenarios

CONCLUSIONS

Monte Carlo-based sensitivity analysis is conducted in order to identify important variation of properties or process and their related parameters accompanied with the early failure of overpack and the alteration of buffer. In the early failure scenario, the integrated changes of glass dissolution rate, effective diffusion coefficients and distribution coefficients in the buffer due to early high temperature have no detrimental effect on Se-79 and Cs-135 maximum release rates for 40,000 vitrified waste canisters from the buffer. However, the 97.5th percentile value of Se-79 in the early failure scenario under the additional condition of increased Se solubility by the radiolysis is about one order of magnitude higher than that in the normal scenario. This result indicates the need to understand the feasibility on the scenario of the increase of Se solubility correlated with the enhanced redox potential due to the radiolysis after the early failure of overpack. Additionally, the 97.5th percentile values of Se-79 and Cs-135 in the alteration scenario of buffer are higher than in the early failure scenarios. These results suggest that the effect of the deterioration of the expected barrier functions relevant to the buffer alteration on Se-79 and Cs-135 release rates is more remarkable than that of early failure of the overpack.

REFERENCES

1. Nuclear Waste Management Organization of Japan (NUMO), "Evaluating Site Suitability for a HLW Repository (Scientific Background and Practical Application of NUMO's Sitting Factors)", NUMO-TR-04-04, NUMO, 2004 (in Japanese).
2. Japan Nuclear Cycle Development Institute (JNC), "H12: Project to Establish the Scientific and

- Technical Basis for HLW Disposal in Japan - Supporting Report 3: Safety Assessment of the Geological Disposal System –“, JNC TN410 2000-004, 2000.
3. Nakayama, G., Akashi, M., “The Critical Condition for Initiation of Localized Corrosion of Mild Steels in Alkaline Water Environment in Contact with Bentonite”, *Zairyo- to - Kankyo*, 49, 222 – 227 (2000) (in Japanese)
 4. Mitsui, H., Takahashi, R., Taniguchi, N., Otsuki, A., Asano, H., Yui, M., “Study on the Corrosion Assessment of Overpack Welds- □ ”, *JAEA-Research 2006-080, RWMC-JRJ-06001*, 2006 (in Japanese)
 5. R. N. Parkins., S. Zhou., “The Stress Corrosion Cracking of C-Mn Steel in CO_2 - HCO_3^- - CO_3^{2-} Solutions. □ □ Stress Corrosion Data”, *Corrosion Science*, Vol.39, No.1, pp.159-173, 1997
 6. Maeda, T., Watanabe, M., Takeda, S., Nakayama, S., “An empirical model to determine the modes of corrosion of carbon steel under near field environments of geological disposal”, *The 13th International Conference on Environmental Remediation and Radioactive Waste Management, ICEM2010 – 40113* (2010)
 7. Nakayama, S., Sakamoto, Y., Yamaguchi, T., Akai, M., Tanaka, T., Sato, T., Iida, Y., “Dissolution of montmorillonite in compacted bentonite by highly alkaline aqueous solutions and diffusivity of hydroxide ions”, *Appl. Clay Sci.* 27, 53–65, 2004.
 8. Yamaguchi, T., Sakamoto, Y., Akai, M., Takazawa, M., Iida, Y., Tanaka, T., Nakayama, S., Experimental and modeling study on long-term alteration of compacted bentonite with alkaline groundwater. *Phys. Chem. Earth* 32, 298-310, 2007.
 9. Takeda, S. and Kimura, H., Uncertainty and Sensitivity Analysis for Long-Term Performance of Sand-Bentonite Buffer Material, *Proceedings of Waste Management Symposia 2010*, 2010.
 10. Takeda, S. and Kimura, H., “Uncertainty Analyses for HLW Disposal System Using Probabilistic Safety Assessment Code (GSRW-PSA): Parameter Uncertainty and Conceptual Model Uncertainty in Natural Barrier”, *JAERI-Research 2002-014*, 2002 (in Japanese).
 11. Takeda, S. and Kimura, H., “Uncertainty Analysis of Solubility for Selenium and Neptunium by Monte Carlo Simulation of Geochemical Modeling Code”, *JAEA-Research 2006-069*, 2006 (in Japanese).
 12. Iman, R. L. and Shortencarier, M. J., “A FORTRAN 77 Program and User’s Guide for the Generation of Latin Hypercube and Random Samples for Use with Computer Models”, *NUREG/CR-3624*, 1984.
 13. Wolery, T. J. “EQ3/6, A Software Package for Geochemical Modeling of Aqueous Systems: Package Overview and Installation Guide (Version 7.0)”, *UCRL-MA-110662 PT I*, 1992.
 14. Olin, A., Nöling, B., Osadchii, E. G., Öhman, L. O., Rosén, E., *Chemical Thermodynamics of Selenium (Chemical Thermodynamics, Vol.7)*, Elsevier Science B.V., Amsterdam, 2005.
 15. Iida, Y., Yamaguchi, T., Tanaka T., Kitamura, A. and Nakayama, S., "Determination of the solubility limiting solid of selenium in the presence of iron under anoxic conditions," *Proc. Mobile Fission and Activation Products in Nuclear Waste Disposal, La Baule, January 16-19, 2007*, 135-145, 2009.
 16. Sekioka, Y., Takeda, S. and Kimura, H., “Study on Uncertainties of Glass Dissolution Rate in Safety Assessment for a Geological Disposal of High Level Radioactive Waste, *JAEA-Research 2009-062*, 2010 (in Japanese).